Real-time Algorithm to Classify AE Events of Lamb Waves in CFRP

Antolino GALLEGO *, José MARTINEZ-JEQUIER **, Elisabet SUÁREZ *,
Francisco J. JUANES ***, Angel VALEA ***
* University of Granada. School of Engineering Building, Granada, Spain
** NDT Ingenieros, Madrid, Spain
*** University of Basque Country, Chemical Engineering and Environmental, Bilbao, Spain

Abstract. Internal damage like delaminations is one of the most critical damage in composite laminates not detectable through visual inspection. Its detection is one of the most attractive challenges in the Structural Health Monitoring. Acoustic Emission is a promising SHM technique for achieving that. AE Lamb waves offer a good approach to evaluate this kind of materials, but due to the combination of different wave propagation modes, reflections, dispersion effects, attenuation and constructive/destructives interferences, its separation becomes a major problem.

It is well known that delamination produces mechanical displacement micro-pulses outside the plane (OP), while matrix micro-cracking and tensile fiber breakage produce micro-pulses inside the plane (IP). Moreover, it has been verified that the A0 mode is favored by OP excitations, while the S0 mode is favored by IP excitations. From these previous assumptions, this work proposes an algorithm to classify the AE events into the three damage mechanisms. However, in general, both modes will be present simultaneously in a particular AE signal, reason why the major issue of the algorithm proposed here consists in an efficient separation of both modes, trying to avoid such a collateral factors as reflections or influence of the threshold used for AE detection.

Algorithm has been entirely implemented using the ECP code of the AEVisual software, so it can be run in real-time. The paper proposes its validation in control tests, in which only a damage mechanism is generated, and also in three-point bending tests of composite samples with and without artificial delaminations supplied by Airbus-Spain.

Introduction

The characteristics of Carbon Fiber-Reinforced Polymer (CFRP) composites have permitted their extensive use in a large variety of applications. Acoustic Emission (AE) testing is an excellent candidate for real-time damage monitoring of loaded CFRP structures because it is able to provide information on damage progression [1].

The plate theory establishes that AE waves propagate through plates in two main modes, the symmetric (S0) and the anti-symmetric (A0) mode [2,3]. Mode separation becomes a major problem in real applications, due to reflections and other physical effects like dispersion, attenuation and constructive/destructive interferences. The separation of these modes enables one to extract information about the damage mechanism [4].

Delamination, usually produced by impact, would constitute critical internal damage in laminate composites, not detectable through visual inspection [4,5]. Its detection during service operations can be seen as an attractive and outstanding challenge. This failure is largely associated with the production of mechanical displacement micro-pulses outside the plane (OP), i.e. source motions perpendicular to the mid-plane of the plate [6,7]. On the other hand, matrix micro-cracking and tensile fiber breakage may produce overall micro-pulses inside the plane (IP), i.e. source motions that are in the plane of the plate and symmetric about the mid-plane [6,7]. Recent work has verified that the A0 mode is favored by OP excitations, while the S0 mode is favored by IP excitations [2].

Our study proposes a new algorithm to classify AE events into the three predominant damage mechanisms in CFRP, by associating the delamination progress to the A0 mode, and the fiber breakage and matrix micro-cracking to the S0 mode. However, in general, due to the microscopic anisotropy of the CFRP, both modes will be present simultaneously in a particular AE signal. That is why the key contribution of the algorithm proposed here consists of an efficient hardware/software separation of both modes, in an attempt to avoid collateral factors such as reflections or any influence of the AE threshold.

In this work, in order to generate each damage mechanism as a sole process, three control tests (delamination test, fiber breakage test and matrix micro-cracking test) were carried out. Moreover, three point bending tests were carried out on four samples extracted from a CFRP plate supplied by Airbus-Spain, with and without induced delaminations.

In particular, the algorithm proposed here considers the use of two hardware filters during acquisition: one in the low-frequency range, LF=[20-55] kHz; and the other one in the high-frequency range, HF=[125-660] kHz. The [55-125] KHz band was filtered out, because in it the A0 and S0 modes propagate simultaneously with reasonable amplitudes at similar frequencies, making frequency discrimination impossible.

Therefore, by comparing the RMS (Root Mean Squared) of the AE signals in both frequency bands, it was possible to classify AE events as OP or IP, and thus segregate the delamination mechanism from the fiber breakage and matrix micro-cracking. By evaluating the spectrum of the AE signals recorded in the HF band, it was found that the energy of signals coming from matrix micro-cracking was mainly concentrated over the third to fourth resonances of the sensor, and from fiber breakage from the fourth resonance on up. The algorithm led to separate the IP into events coming from each mechanism separately.

Another important aspect is the use of the RMS energy of the signal calculated only over very narrow time windows near the threshold crossing time. This novel approach meant overcoming the influence of reflections and mode conversion effects. That narrow time windows do not cover the whole range of A0 and S0 transient signals, but they are sufficient and representative ensuring that previous physical assumptions are fulfilled.

A general scheme of the AE signal analysis algorithm, using two classifying steps (hardware and software) is shown in Fig. 1. It was entirely developed in programming language LUA so that it might easily be encapsulated into AE commercial software for real-time applications.

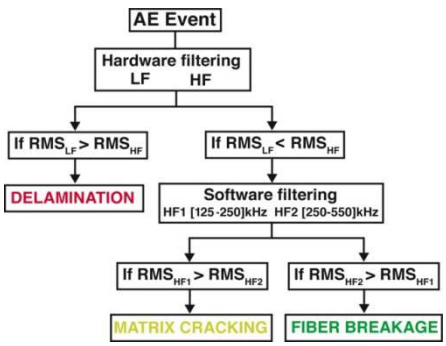

Fig. 1. General scheme of the algorithm proposed.

1. Previous experiments: Mode detection with pencil lead breakage (PLB)

To verify the existence of Lamb waves, PLBs were carried out on a sample plate (281x279 mm) cut from a larger quasi-orthotropic plate, of thickness 4.22 mm and 22 plies, supplied by Airbus-Spain. An oscilloscope was used as the acquisition equipment for the AE signals. Two multi-resonant VS45H sensors (sensitivity response given in Fig. 2-a) were located 90 mm from the top of the sample, at the same point but on opposite sides of the plate, following the technique described in [2] (Fig. 2-b). Several PLBs were carried out, both on the plane of the plate and on the edge, respectively simulating IP and OP sources.

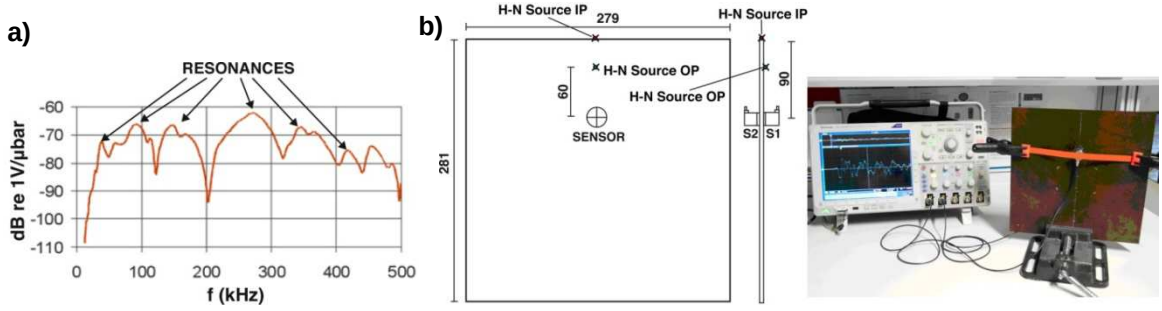

Fig. 2. a) Sensitivity response of the VS45H sensors used in the experiments. **b)** Lamb modes detection experimental scheme. Distances in mm.

Figure 3 (left) shows the original signals –without any filtering– recorded in both cases; and although both modes are visually recognizable (S1 and S2 signals are in phase for S0 mode or in opposite phase for A0 mode) figuring individual separation calls for extra data treatment. To this end digital filtering with MATLAB commercial software was performed off line, considering two frequency bands.

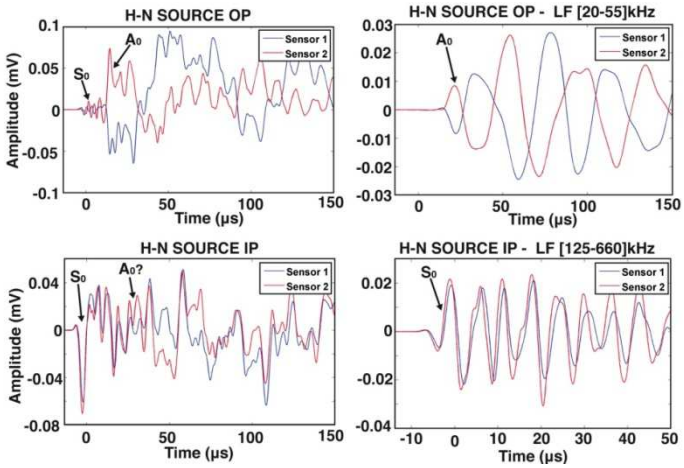

Fig. 3. Original (left) and filtered (right) signals from the Lamb modes detection experiment.

One band in the low frequency range to capture mainly the A0 mode corresponds to the first resonance of the sensor (LF=[20-55] kHz) and the other in the high frequency range to capture mainly the S0 mode corresponds to the third resonance and up (> 3rd attenuated by propagation along the 90 mm distance to sensor) (HF=[125-660] kHz). These filters generate very effective separation of two modes.

2. Configuration setup and tests

A Vallen AMSY-5 was used as the acquisition equipment. In all tests, the signal was injected into and recorded simultaneously in five independent channels, with different input frequency filters and thresholds configured in each (see Fig. 4).

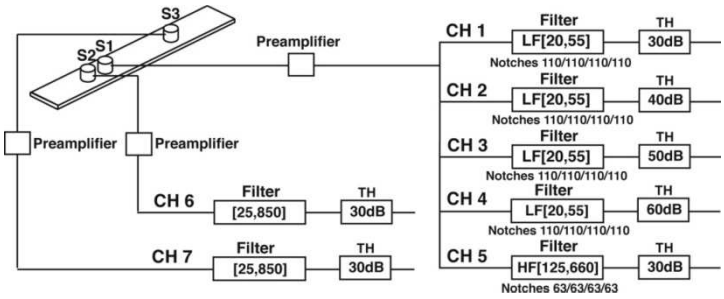

Fig. 4. AE experimental setup. Channels, filters and thresholds scheme used in bending and control tests.

2.1. Delamination test

An already existent delamination was forced to grow in a pre-delaminated sample involving two loading periods, two load holds, and a final unloading (see Fig. 5-a). Fig. 5-b, shows two AE signals from the same hit recorded with the LF-CH2 and HF-CH5 channels. The S0 mode is seen to still propagate at the low frequency, but with a much lower energy than the A0 mode. However, using a threshold of 40 dB (i.e. by selecting the channel CH2) it is possible to discard the S0 mode and capture only the genuine A0 mode itself after the Threshold Crossing (THC). It can also be seen that the amplitude of the A0 mode of the LF channel is much greater than its corresponding HF amplitude (CH5), confirming that it was originated by OP micro-displacement.

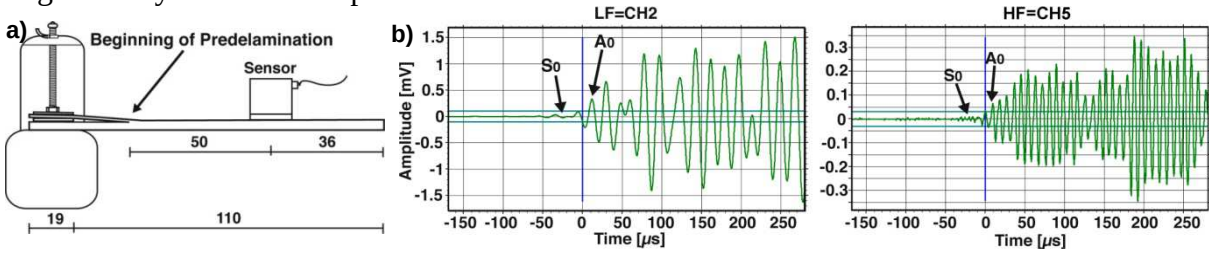

Fig. 5. a) Delamination test scheme. **b)** AE signals from the same event recorded during the delamination test. Centre: LF (CH2); Right: HF (CH5).

2.2. Fiber breaking test

This control test was carried out by introducing and gluing fiber bundles in between two of the carbon fiber layers of a pre-delaminated sample and pulling them out to breakage. Obviously, boundary conditions are different than in the case of a fiber confined within the epoxy matrix, but this is an acceptable approach. In this case, very repetitive short duration AE signals were recorded with CH5, confirming that this mechanism mainly produces HF energy. The spectrum in the post-trigger window [-2,4] µs (Fig. 6-a) reveals that this mechanism mainly generates HF energy over 300-500 kHz.

2.3. Matrix micro-cracking test

A sample of graphite epoxy resin having the same sizes as the CFRP samples used in the bending tests was manufactured. The test consisted of generating AE activity in the epoxy resin sample under stress by subjecting it to acetone, which chemically degrades, causing surface micro-cracking in the resin. In this case, the amplitudes of the AE signals recorded were not higher than 50 dB. Moreover, signals recorded by the HF channel (CH5) had much larger amplitudes than the signals recorded in the LF channels, confirming once again that this mechanism mainly produces HF energy. Figure 6-b shows the frequency spectrum in the post-trigger window [-2,4] µs, revealing that this mechanism mainly generates HF energy around 250 kHz, near the fourth sensor resonance.

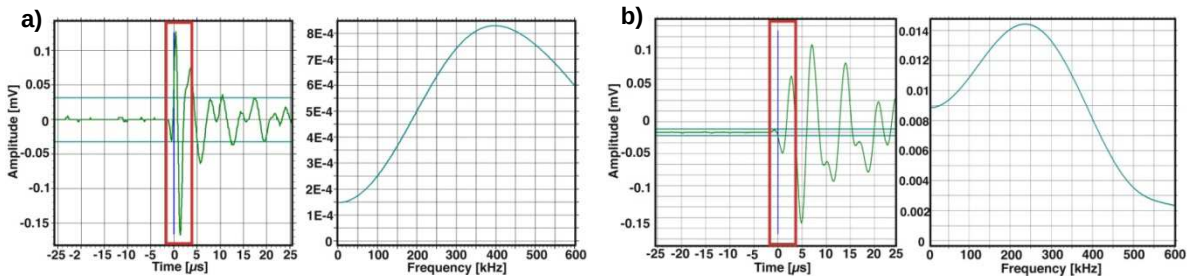

Fig. 6. a) Fiber breakage control test; **b)** Matrix micro-cracking test. Left: Temporal signal recorded. Right: Spectral response in the time window [-2,4] μs.

2.4. Three point bending tests

Four samples sized 260x40 mm^2 were cut from a CFRP plate supplied by Airbus-Spain. The samples designated as SD and BD were deliberately pre-delaminated at a specific location by inserting a Teflon film between two layers, the respective sizes being 25x25 mm^2 (SD) and 40x50 mm^2 (BD). The other two samples, ND1 and ND2, were left without any pre-delamination. A three point bending test (with a displacement velocity of 0.5 mm/min) was carried out to induce all kinds of damage mechanisms. Two guard sensors, S2 and S3, were used. The breaking load of the samples was 237.7 kg for ND1, 260.24 kg for ND2, 233.5 kg for SD and 192.35 kg for BD, confirming that the previous existence of a delamination leads to a loss in strength of the material.

3. Data Analysis

AE hits with amplitudes lower than 45 dB were not considered due to the difficulty of matching the time window to the first signal appearances. Signals were grouped as: **H1**: One-hit events corresponding to the HF channel (CH5); **L1**: One-hit events corresponding to any LF channel; **HS**: Events with subsequent hits, the HF channel being the first-hit channel; **LS**: Events with subsequent hits, any LF channel being the first-hit channel.

After detailed observation of the signals, the window W_{LF}=[0,22] μs was selected to calculate the RMS of the signals recorded in LF channels (RMS_{LF}). It was corroborated that this window mainly avoids the presence of reflections and mode conversions, properly capturing the genuine A0 mode. Then, in order to select the proper LF channel (CH1, CH2, CH3 or CH4), the following criteria were used: **CH1:** if A≤45; **CH2** if 45<A≤60; **CH3** if 60<A≤80; **CH4** if A>80. As confirmed, this dynamic criterion for the LF channel enabled us to properly capture a substantial and significant part of the A0 mode. As an example, Fig. 7 shows a signal with peak amplitude A=76.1 dB recorded by the LF channels CH1, CH2 and CH3. It can be seen that with the selected channel CH3, based on the above criterion, a significant part of A0 mode is properly picked up. Note that the choice of channels CH1 or CH2 would have delivered erroneous results.

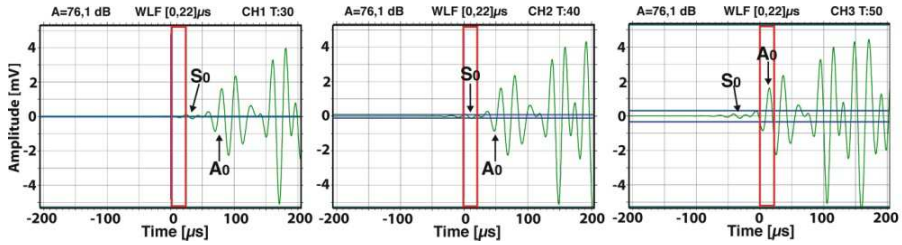

Fig. 7. LF window. Transient recordings of a 76.1 dB peak amplitude signal at CH1, CH2 and CH3.

For signals recorded with the only HF channel, two temporal windows were defined to capture the S0 mode: a post-trigger (after the THC) window W_{HF1}=[-2,4] µs; and a pre-trigger (before the THC) window W_{HF2}=[-7,-1] µs. For each HF signal, the RMS energy in both windows was calculated, hence RMS_{HF1} and RMS_{HF2}. By comparing RMS_{HF1} and RMS_{HF2}, an automatic decision was implemented in the algorithm to select which window would best capture the S0 mode in each event without a significant influence of reflections.

Once the RMS_{LF} and RMS_{HF} were calculated for each event, the algorithm (Fig. 8) was applied to associate each event to a specific class of damage. The following designation was used: Matrix micro-cracking (**Dela=0**); Delamination (**Dela=1**); Fiber breakage (**Dela=2**). The decision algorithm obviously depends as well on event features:

-For L1 and LS events: They were directly classified as Dela=1 because no signal or a weaker signal was recorded in the HF channel. It was thus assumed that most of their energy corresponded to the A0 mode.

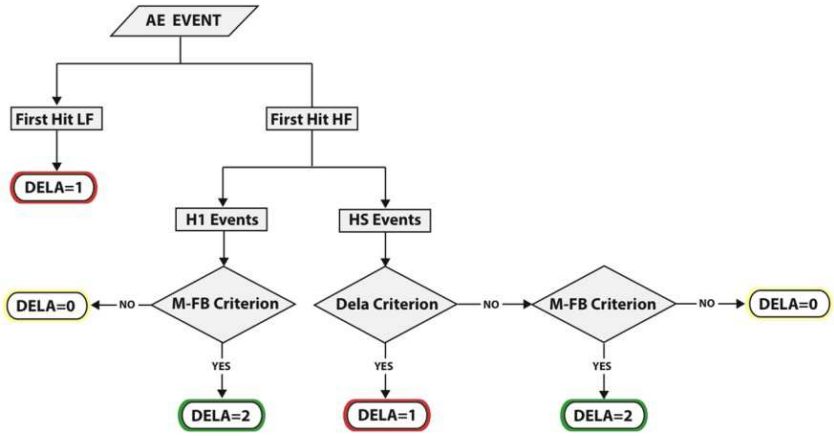

Fig. 8. Block diagram of the algorithm for damage mechanisms segregation.

-For H1 events: Due to the fact that no signal was received in the LF channel, these events were associated to IP micro-displacements, since most energy would correspond to the S0 mode. Thus, the events were associated to mechanism Dela=0 or Dela=2, according to a specific spectral criterion (**M-FB criterion**) proposed.

The Spectral Ratios (SR) of the HF signal in the window W_{HF} were calculated over three individual bands corresponding to three resonances of the sensor: BW1=[125-250] kHz (third resonance); BW2=[250-350] kHz (fourth resonance); BW3=[350-550] kHz (fifth resonance). To avoid spectral distortions delivering unreliable results, the spectral ratios of BW2 and BW3 were gathered and calculated as the individual sum of the two bands. The rate of the SR between these bands (BW2, BW3) and BW1, in dB, is given by:

$$R_{SR_{HF}} = 20\log\left[10^{\frac{SR_{HF_{BW2}}}{20}} + 10^{\frac{SR_{HF_{BW3}}}{20}}\right] - SR_{HF_{BW1}} \quad (1)$$

Bearing in mind that fiber breakage emission falls mainly within the fourth and fifth resonances [BW2 and BW3], if $R_{SR_{HF}}$ was higher than a particular threshold T_{SR}, the event was associated with Dela=2. Otherwise, the event was associated with Dela=0.

-For HS events: In this case, since events have LF and HF signals, to associate those events with IP or OP micro-displacements, the difference of the RMS value in LF and HF was calculated **(Dela Criterion)**, i.e.

$$R_{LF-HF} = RMS_{LF} - RMS_{HF} \quad (2)$$

Thus, if $R_{LF-HF} \geq 0$, the event has more energy in LF than in HF, so it was associated with OP micro-displacements (Dela=1). Otherwise, the event was associated with IP micro-displacements and the **M-FB criterion** was applied to associate it with Dela=0 or Dela=2.

4. Results of control tests

Firstly, the algorithm was applied to the AE signals coming from the control tests. For the delamination test in particular, most events were correctly classified as Dela=1, both in loading, load holds and unloading (see Fig. 9-a). Indeed, the variable R_{LF-HF} used to classify the HS events was greater than 10 dB for more than 95% of HS events. Validation was also clearly verified for the fiber breakage control test, in which case 100% of the events were classified as Dela=2 (Fig. 9-b). In this case, the variable $R_{SR_{HF}}$ (used to discern between Dela=0 and Dela=2) was consistently higher than 11 dB, demonstrating that most of the energy emitted by this mechanism falls into the frequency band BW2-BW3=[250-550] kHz. For the matrix micro-cracking control test, meanwhile, most of the events were classified as Dela=0 (see Fig. 9-c), proving that the energy emitted in this mechanism remained in the frequency band BW1=[125-250] kHz. In this case, the variable $R_{SR_{HF}}$ had values that were always less than 9 dB.

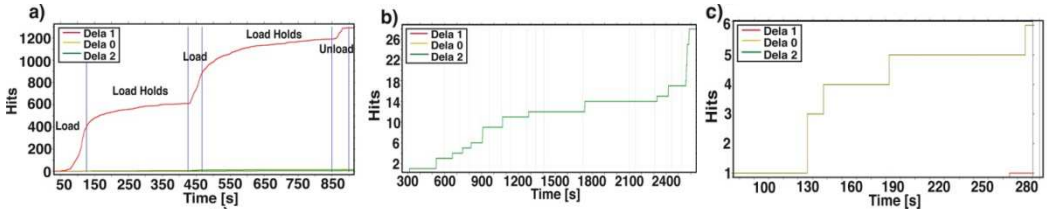

Fig. 9. Classification of AE events in the control-tests: **a)** Delamination test; **b)** Fiber-breakage test; **c)** Matrix micro-cracking test.

These control tests also allowed us to determine the threshold T_{SR} finally proposed for criterion M-FB. Taking into account that R_{SRHF} was always higher than 11 dB in the fiber breakage control tests and less than 9 dB in the matrix micro-cracking control test, a value of T_{SR}=9 dB was established to arrive at a correct classification of events in both cases.

5. Results of three point bending tests

SD (Small Delamination) and BD (Broad Delamination) samples

For the pre-delaminated samples subjected to bending tests, SD and BD, most events were associated to Dela=1. Events appeared almost from the beginning (10% of breaking load for the BD and 20% for the SD). It was visually evident that sample BD broke only by delamination, given that the pre-delamination occurred along the whole width of the sample. This could be clearly corroborated because no significant increase in the Dela=0 and Dela=2 mechanisms was seen at any time (see Fig. 10-a). In contrast, sample SD showed a sudden, substantial and sustained increase of the Dela=1 slope at 80% of load, very possibly related to the generation of a new delamination, followed a bit later by an increase in the Dela=0 rate. Moreover, a significant increase in the Dela=2 events is observed around 93% of load, announcing the final breaking of the sample (see Fig. 10-b).

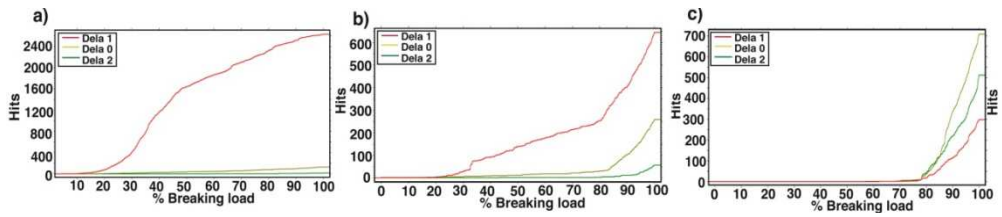

Fig. 10. Three point bending test results: **a)** BD; **b)** SD; **c)** ND1.

ND1 and ND2 samples (No Delamination)

Figure 10-c refers to sample ND1. It shows a totally different behavior than the preceding pre-delaminated samples. AE onset was established at 57% of break load in the absence of a pre-delamination. From this point, all three mechanisms began to increase slowly, meaning that Dela=1 was not the prevailing type of event, in contrast with the pre-delaminated samples. At 79% of break load a significant increase of all three mechanisms took place. In this case, two delaminations were visually observed, matching the two different slope increases of the Dela=1 events (at 79% and 92% of break load). The behavior of the sample ND2 was very similar to that seen for ND1. In this case, the AE events started at 62% of the break load. A significant increase in Dela=0 and Dela=2 was witnessed at 77% of break load, marking the onset of delamination. A sudden increase in Dela=1 and Dela=0 events at 87% of ultimate load coincides with a considerable increase of the delamination in course. It must also be stressed that the onset of significant delamination in samples ND1 and ND2 appeared at the same value of load (77%) as the onset of the second delamination in the pre-delaminated sample SD.

6. Conclusions

A new procedure to evaluate, in real-time, the progress of delaminations in CFRP composite plates using the acoustic emission technique has been proposed. It entails an algorithm based on an appropriate separation between the S0 and A0 Lamb modes in the AE signals. Firstly, two hardware filters were used during acquisition: LF=[20-55] kHz to capture mainly the A0 mode, and HF=[125-660] kHz to capture mainly the S0 mode. Secondly, by comparing the strength of the AE signals in the two frequency bands in very narrow windows, it was possible to classify AE events as outside or inside the plane, and thus segregate the delamination mechanism from other ones. Thirdly, the Spectral Ratio made it possible to separate the AE events coming from matrix micro-cracking and the fiber breaking mechanisms. The use of very narrow temporal windows is an original contribution of this paper, and allows for a comparative evaluation of the genuine strength of S0 and A0, significantly mitigating the influence of reflections and other secondary propagation effects. Sensors were also properly selected to ensure the necessary sensitivity in the HF and LF ranges used in this experimental work.

References

[1] Ono K, Gallego A. Research and application of AE on advanced composite. Journal of Acoustic Emission 2012; 30: 180-229.
[2] Ono K, Gallego A. Attenuation of Lamb waves in CFRP plates. Journal of Acoustic Emission 2012; 30: 109-123.
[3] Guo D, Mal A, Ono K. Wave theory of acoustic emission in composite laminates. Journal of Acoustic Emission 1997; 15: 14-19.
[4] Ip HK, Mai, WY. Delamination detection in smart composite beams using Lamb waves, Journal of Smart Materials and Structures 2004; 13: 544-551.
[5] Sridharan S. Delamination behavior of composites. Woodhead Publishing; 2008.
[6] Mizutani Y, Nagashima K, Takemoto M, Ono K. Fracture mechanism characterization of cross-ply carbon-fiber composites using acoustic emission analysis. NDT&E International 2000; 33: 101-110.
[7] Prosser WH, Jackson KE, Kellas S, Smith BT, MacKaon J, Friedman A. Advanced waveform based acoustic emission detection of matrix cracking in composites. Materials Evaluation 1995; 53: 1052-1058.